Solution of some inverse problems for heat and mass transport in unsaturated porous media

JOZEF KAČUR
Slovak University of Technology
Department of Physics
Radlinského 11, 810 05 Bratislava
SLOVAKIA
Jozef.Kacur@fmph.uniba.sk

PATRIK MIHALA
Comenius University
Department of MANM
Mlynská dolina, 842 48 Bratislava
SLOVAKIA
pmihala@gmail.com

MICHAL TÓTH
Comenius University
Department of MANM
Mlynská dolina, 842 48 Bratislava
SLOVAKIA
m.toth82@gmail.com

Abstract: We discuss the numerical modeling of heat and water transport in unsaturated-saturated porous media with heat exchange between the infiltrated water and porous media matrix. An unsaturated-saturated flow is considered with boundary conditions reflecting the external driven forces. The developed numerical method is efficient and can be used for solving inverse problems concerning determination of hydraulic soil parameters, dispersion coefficients and transmission coefficients for heat energy exchange. Numerical experiments support our method.

Key–Words: porous media infiltration; water and heat transport; heat energy exchange; numerical modeling of nonlinear system

1 Introduction

In this contribution we discuss the heat transported by infiltrated water into porous media taking into account the heat exchange between infiltrated water and the porous media matrix assuming the flow is unsaturated. This is motivated by an analysis of hygrothermal insulation properties of building facades. The influence of external weather conditions is included in the considered model. We focus especially on the determination of model parameters in a complex mathematical model. Solution of corresponding inverse problems relies on measurements in laboratory conditions using real 3D samples.

The mathematical model consists of the coupled system of strongly nonlinear PDE of elliptic-parabolic type. The flow of water in unsaturated-saturated porous media is governed by Richard's equation. The heat energy transported by infiltrated water is subject to the convection, molecular diffusion, and dispersion, which are driven by external forces due to water and heat fluxes caused by weather conditions. Mathematical models are well known and presented in many monographs, e.g., [1], with very complex list of quotations. Fundamentals of heat and mass transfer with many applications are discussed in [9]. In our setting the heat energy transmission from water in pores to the porous media matrix is treated analogously to the reversible adsorption of contaminant in unsaturated porous media, see e.g. [8],[2]. Additionally, we take into account the heat conduction of the porous media matrix itself. Thus, soluted contaminant in water is replaced by heat energy. Solving the heat conduction of porous media (without water in pores) is difficult task and is modeled by homogenization method. In our setting we assume very simple heat conduction in matrix, where heat permeability is obtained separately by solving a corresponding inverse problem and using practical measurements. We also determine both transmission coefficient and heat permeability in matrix via the solution of the inverse problem.

Recently, we have discussed in [6] determination of soil parameters in porous media flow model, based on empirical van Genuchten/Mualem capillary/pressure model. There, we have used radially symmetric 3D sample using inflow/outflow measurements. The main reason was that 1D samples (in form of thin tubes) used before suffer from preferential stream lines arising in experiments, especially using centrifugation. We have significantly eliminated this effect by suitable infiltration scenario with cylindrical sample, where infiltration flux from sample mantle is orthogonal to gravitational force. Moreover, the infiltration area is substantially larger then the area of the top of the tube. Thus, we obtained more reliable results in determination of soil parameters. In figure 1 we sketch the cylinder sample used in experiments.

In this manuscript we present the experiment scenarios to determine dispersion coefficients and successively also heat exchange parameters: transmission and heat conduction coefficients. To determine dispersion coefficients we suggest the following experiment scenario. We assume the inflow/outflow concentration

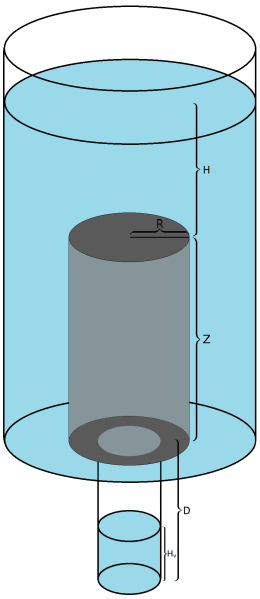

Figure 1: Sample

of a tracer in the infiltrated water that is perfectly dissolved in the water and not adsorbed by the porous media matrix. We assume that the concentration of a suitable tracer can be characterized by means of the electrical resistance. Then transient measurements of electrical resistance of cumulated outflow water could be used. Such a tracer has been used in [4]. The concentration measurement of cumulated outflow water is the main information used for determination of dispersion coefficients.

The heat energy exchange is modeled by temperature gap, water saturation and transmission coefficient. It is almost impossible to measure the temperature gap between the water in pores and in matrix inside the porous media, but we can measure the consequences of heat energy exchange. In our contribution we propose a suitable experimental scenario, which allows the determination of required model parameters using relatively simple measurements. The cylindrical sample is initially uniformly low saturated (almost dry). The temperature of water and matrix is the same, e.g. 20°C. Then we let to infiltrate water (through the cylinder mantle) with lower temperature, e.g., 0°C. The top and bottom boundary of the cylinder are isolated. We measure the time evolution of temperature in the middle of the top of the cylinder. We note that temperatures of water and matrix in this point (even on whole axis of the cylinder) are the same for long time interval in experiment. The reason is that the infiltrating water has a very sharp front and slowly progresses towards the cylinder axis. Simultaneously the heat is conducted by the matrix and due to the heat exchange the temperature of water and the matrix are almost the same in the neighborhood of the axis and decrease. This observation is supported by our numerical experiments. Thus, the time evolution of temperature in the top point of axis is the main information in determination of transmission coefficient and, moreover, also heat conduction coefficient of the matrix.

In this model setting we do not assume the temperature influence on the water flow, but it could be included. However, the heat transport and its mutual transmission with the porous matrix strongly depend on the water saturation in pores.

In the heat and mass transfer problem in facades we consider 2D problem which represents a cross-section of the facade. The parallel vertical boundaries of the rectangle represent the building and outdoor environment contacts.

In the numerical method we use operator splitting method where we successively along small time interval separately solve water flow, then heat transport in water and then in matrix including heat exchange. In the solution of water flow we follow the approximation strategy introduced in [5] and also used in well known software Hydrus (see [3]). To control the correctness of our numerical results we have developed also an approximation scheme (see [8] used only for 1D) based on the reduction of the governing parabolic equations to a stiff system of ordinary differential equations. This approximation solves simultaneously whole system, but computational time is significantly larger. The main reason is that the system is stiff and too large when using necessary space discretization. Comparisons justify our method which is significantly quicker and therefore applicable in the solution of inverse problems in mathematical model scaling. Moreover, present method could be efficiently used also for solving 3D problems.

2 Mathematical Model

2.1 Water Flow Model

Water saturation $\theta \in (\theta_r, \theta_s)$ (θ_r is irreducible saturation and θ_s is porosity) is rescaled to effective saturation

$$\theta_{ef}(h) = \frac{\theta(h) - \theta_r}{\theta_s - \theta_r}.$$

Here, h ([cm]) is hydraulic head and the fundamental empirical relation between saturation θ and h in terms of van Genuchten/Mualem empirical model (capillary/pressure law) is

$$\theta(h) = \theta_r + \frac{\theta_s - \theta_r}{(1 + (\alpha h)^n)^m},\ \theta_{ef}(h) = 1 \quad (1)$$

for $h \geq 0$. Hydraulic permeability K is modeled by

$$K(h) = K_s k(\theta_{ef}),\ \ k(\theta_{ef}) = \theta_{ef}^{\frac{1}{2}}(1-(1-\theta_{ef}^{\frac{1}{m}})^m)^2, \tag{2}$$

where K_s is hydraulic permeability for fully saturated porous media. Water flux $\vec{q}$

$$\vec{q} = (q^x, q^y), \quad \vec{q}(h) = -K(h)(\nabla h - e_y),$$

where e_y is a unit vector in direction y representing gravitational driving force. Richards equation is of the form

$$\partial_t \theta(h) - div(K(h)(\nabla h - e_y)) = 0 \tag{3}$$

with the corresponding boundary conditions which will be specified in numerical experiments section.

2.2 Heat Energy in the Water

Conservation of water heat energy is expressed in PDE

$$c_v \partial_t(\theta T_w) - div(-c_v \vec{q} T_w + \underbrace{(D_o\theta + \bar{D})}_{D} \nabla T_w) = \sigma\theta(T_w - T_m) \tag{4}$$

where T_w is temperature of water, c_v is heat capacity of unite water volume, σ is transmission coefficient of the heat exchange with the matrix. The heat energy flux is

$$\vec{QT} = -c_v \vec{q} T_w + \underbrace{(D_o\theta + \bar{D})}_{D} \nabla T_w.$$

Convective part is $c_v \vec{q} T_w$ and the diffusion/dispersion are characterized by molecular diffusion coefficient D_o and dispersion matrix $\bar{D}$, where

$$\bar{D} = \begin{pmatrix} D_{1,1} & D_{1,2} \\ D_{2,1} & D_{2,2} \end{pmatrix} = \frac{1}{|\vec{q}|} \times \begin{pmatrix} \alpha_L((q^x)^2 + \alpha_T((q^y)^2 & (\alpha_L - \alpha_T)(q^x q^y) \\ (\alpha_L - \alpha_T)(q^x q^y) & \alpha_L((q^y)^2 + \alpha_T((q^x)^2 \end{pmatrix}.$$

Here, α_L, α_T are longitudinal and transversal dispersion coefficients. The corresponding initial and boundary conditions will be specified in the numerical experiments section.

2.3 Heat Conduction in the Matrix

We assume the simple heat conduction model in the matrix

$$c_m \partial_t T_m - \lambda \Delta T_m = \sigma\theta(T_w - T_m) \tag{5}$$

where T_m - matrix temperature, λ - heat conduction coefficient and c_m- heat capacity of the matrix.

2.4 Boundary Conditions

Our solution domain Ω is a rectangle $(x, y) \in (0, X) \times (0, Y)$ with $X = 5, Y = 10$. We consider the following boundary and initial conditions

$$\begin{aligned} &\partial_y T_m = 0, \quad QT^y = 0, \quad h = h_0 \\ &\text{on } (0, X) \times \{0\} \times (0, \Upsilon) \\ &\partial_y T_m = 0, \quad QT^y = 0, \quad q^y = 0 \\ &\text{on } (0, X) \times \{Y\} \times (0, \Upsilon) \\ &T_m = 20, \quad T_w = 20, \quad h = -200 \\ &\text{on } (0, X) \times (0, Y) \times \{0\}, \end{aligned}$$

on $\{X\} \times (0, Y) \times (0, \Upsilon)$

$$\begin{aligned} \partial_x T_m &= \sigma_{m,r}(TM_r - T_m), \\ QT^x &= \sigma_{w,r}(TW_r - T_m), \\ q^x &= \sigma_{ww,r}(HW_r - h) \end{aligned}$$

and on $\{0\} \times (0, Y) \times (0, \Upsilon)$

$$\begin{aligned} -\partial_x T_m &= \sigma_{m,l}(TM_l - T_m), \\ -QT^x &= \sigma_{w,l}(TW_l - T_w), \\ -q^x &= \sigma_{ww,l}(HW_l - h), \end{aligned}$$

where TM, TW, TH are external temperature and pressure sources, and $\sigma_{.,r}$, $\sigma_{.,l}$ are corresponding boundary transmission coefficients. In our numerical experiments we consider on the right boundary the hydrostatic pressure $h = (Y - y), y \in (0, Y)$. Also the boundary flux conditions could be changed to Dirichlet boundary conditions.

2.5 Mathematical Model in Cylindrical Coordinates

Consider the cylinder with radius R and height Y. Using cylindrical coordinates (r, y) in (3), (4) , (5) we obtain

$$\partial_t \theta(h) = \frac{1}{r}\partial_r(rK(h)\partial_r h) + \partial_y(K(h)(\partial_y h - 1)) \tag{6}$$

for water flow

$$c_v \partial_t(\theta T_w) - \left(\frac{1}{r}\partial_r(rQT^r) + \partial_y(QT^y)\right) = \sigma\theta(T_w - T_m) \tag{7}$$

for heat transport in water and

$$c_m \partial_t T_m - \lambda\left(\frac{1}{r}\partial_r(rQT_m^r) + \partial_y(\partial_y T_m)\right) = \sigma\theta(T_w - T_m).$$

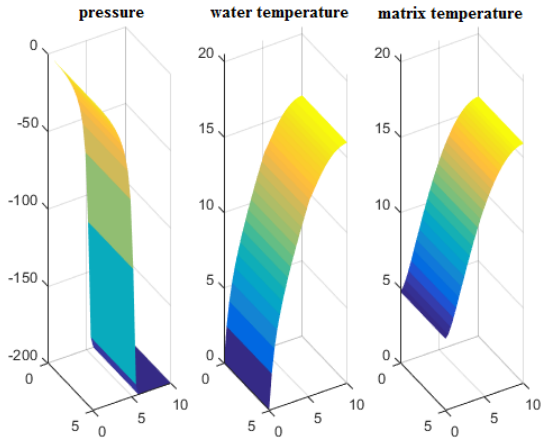

Figure 2: Water pressure h and temperatures T_w, T_m at $t = 500s$

for heat conduction in the matrix, where

$$\mathbf{q} = -(q^r, q^y)^T, \tag{8}$$

$$q^r = K(h)\partial_r h,\ q^y = K(h)(\partial_z h - 1),$$

$$QT^r = -q^r T_w + \theta(D_{1,1}\partial_r T_w + D_{1,2}\partial_y T_w + D_o\theta, \tag{9}$$

$$QT^y = -q^y T_w + \theta(D_{2,1}\partial_r T_w + D_{2,2}\partial_y T_w + D_o\theta, \tag{10}$$

and $QT^r = \partial_r T_m$.

3 Model Data and Corresponding Numerical Solution

In our numerical experiments we assume the following model data ([CGS] units)

as "standard data" : $\theta_0 = 0.38$, $\theta_r = 0$, $K_s = 2.4\ 10^{-4}$, $\alpha = 0.0189$, $n = 2.81$, $D_o = 0.03$, $\lambda = 0.03$, $\alpha_L = 1$, $\alpha_T = \frac{1}{10}$, $c_v = c_m = 1$ and $\sigma = 0.1$. These data correspond to a limestone.
The boundaries $0 \times (0, 10)$ and $5 \times (0, 10)$ are isolated, i.e. $q^x = 0$ and $\sigma_t = \sigma_m = 0$. On the boundary $(0, 5) \times 0$ (bottom) is prescribed pressure $h = 0$ (infiltration) and temperature $T_w = 0$. On the top $(0, 5) \times 10$ we consider $\partial_y h = 0$ (free outflow) and $\partial_y T_w = 0$. Porous media matrix is on all parts of the boundary isolated. We consider initial conditions $h = -200$, $T_w = T_m = 20$. In numerical experiments we consider uniform partition of the domain with $(N_x, N_y) = (31, 31)$ grid points $(x_i, y_j) = (i\Delta x, j\Delta y)$, $i, j = 0, 1, ..., 30$, $\Delta x = \frac{X}{N_x - 1}, \Delta y = \frac{Y}{N_y - 1}$. The solution is drawn in figure 2.

In the figure 3 we draw flow and temperature fields for the cross-section in cylinder at the time section $t = 60s$ with the modified model data. The water is infiltrated from the mantle of the cylinder under the hydraulic pressure. Here $R = 10$, $Y = 10$. Other conditions are the same as in previous figure for facade.

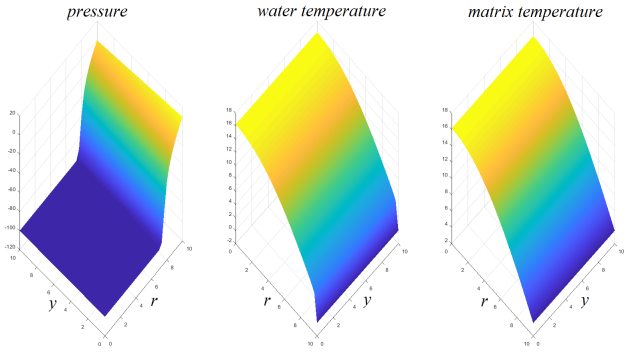

Figure 3: Water pressure h and temperatures T_w, T_m in cylinder at $t = 60s$

4 Numerical Method

In our approximation scheme we apply a flexible time stepping and a finite volume method in space variables. The time derivative we approximate by backwards difference and then we integrate our system over the control volume $V_{i,j}$ with the corners $x_{i\pm\frac{1}{2}}, y_{j\pm\frac{1}{2}}$ and with the length of the edges $(\Delta x, \Delta y)$. Then, our approximation linked with the inner grid point (x_i, y_j) at the time $t = t_k$ is

$$\begin{aligned}
&\Delta x\Delta y\frac{\theta(h) - \theta(h^{k-1})}{\tau} \\
&- \Delta y\left[\frac{K(h_{i+1}) + K(h)}{2}\left(\frac{h_{i+1} - h}{\Delta x}\right)\right] \\
&+ \Delta y\left[\frac{K(h) + K(h_{i-1})}{2}\left(\frac{h - h_{i-1}}{\Delta x}\right)\right] \\
&- \Delta x\left[\frac{K(h_{j+1}) + K(h)}{2}\left(\frac{h_{j+1} - h}{\Delta y} - 1\right)\right] \\
&+ \Delta x\left[\frac{K(h) + K(h_{j-1})}{2}\left(\frac{h - h_{j-1}}{\Delta y} - 1\right)\right] = 0.
\end{aligned}$$

Omitted indices are of values $\{i, j, k\}$.

4.1 Quasi-Newton Linearization

In each (x_i, y_j) we linearize θ in terms of h iteratively (with iteration parameter l) following [Cellia at all][5] in the following way

$$\frac{\theta(h^{k,l+1}) - \theta(h^{k-1})}{\tau} =$$

$$C^{k,l}\frac{h^{k,l+1}-h^{k,l}}{\tau}+\frac{\theta^{k,l}-\theta^{k-1}}{\tau}, \qquad (11)$$

where

$$C^{k,l}=\frac{\partial\theta^{k,l}}{\partial h^{k,l}}=$$

$$(\theta_s-\theta_r)(1-n)\alpha(\alpha h^{k,l})^{n-1}(1+(\alpha h^{k,l})^n)^{-(m+1)}$$

for $h^{k,l}<0$, else $C^{k,l}=0$. We stop iterations for $l=l^*$, when

$$|h^{k,l^*}-h^{k,l^*-1}|\le Tolerance$$

and then we put $h^k:=h^{k,l^*}$.
Finally, we replace the non-linear term $K(h^k)$ by $K(h^{k,l})$. Our approximation scheme then becomes linear in terms of $h^{k,l+1}$. Generally, we speed up the iteration by a special construction of starting point $h^{k,0}\approx h^{k-1}$ and eventually using suitable damping parameter in solving corresponding linearized system. The complex system is solved by **operator splitting method**. To obtain an approximate solution for temperatures in water and matrix at the time section $t=t_k$, starting from $t=t_{k-1}$ we use flow characteristics obtained at $t=t_k$ for $\theta^k, h^k, \vec{q}^k$, and D^k.

4.2 Approximation Scheme for Water Temperature

For $T_w(\equiv T), T_m$ at (x_i,y_j) for $t=t_k$ we obtain by finite volume

$$c_v\theta\frac{T-T^{k-1}}{\tau}\Delta x\Delta y-\Delta y\left[-c_v q^x_{i+\frac12}\frac{T_{i+1}+T_i}{2}+\right.$$
$$D_{1,1,i+\frac12}\frac{T_{i+1}-T_i}{\Delta x}+$$
$$\left.D_{1,2,i+\frac12}\frac{T_{i+1,j+1}+T_{i,j+1}-T_{i+1,j-1}-T_{i,j-1}}{4\Delta y}\right]$$
$$+\Delta y\left[-c_v q^x_{i-\frac12}\frac{T_i+T_{i-1}}{2}+D_{1,1,i-\frac12}\frac{T_i-T_{i-1}}{\Delta x}\right.$$
$$\left.+D_{1,2,i-\frac12}\frac{T_{i,j+1}+T_{i-1,j+1}-T_{i,j-1}-T_{i-1,j-1}}{4\Delta y}\right]$$
$$-\Delta x\left[-c_v q^y_{j+\frac12}\frac{T_{j+1}+T_j}{2}+D_{2,2,j+\frac12}\frac{T_{j+1}-T_j}{\Delta y}\right.$$
$$\left.+D_{2,1,j+\frac12}\frac{T_{i+1,j+1}+T_{i+1,j}-T_{i-1,j+1}-T_{i-1,j}}{4\Delta x}\right]$$
$$+\Delta x\left[-c_v q^y_{j-\frac12}\frac{T_j+T_{j-1}}{2}+D_{2,2,j-\frac12}\frac{T_j-T_{j-1}}{\Delta y}\right.$$
$$\left.+D_{2,1,j-\frac12}\frac{T_{i+1,j}+T_{i+1,j-1}-T_{i-1,j}-T_{i-1,j-1}}{4\Delta x}\right]$$
$$=\Delta x\Delta y\sigma\theta^k(T_m-T_w).$$

4.3 Approximation of $\vec{q}$ and D in Middle Points

We approximate $\vec{q}$ and D in middle points by

$$q^x_{i\pm\frac12}=-\frac{K(h_{i\pm1})+K(h_i)}{2}\left(\frac{\pm h_{i\pm1}\mp h_i}{\Delta x}\right),$$
$$q^y_{j\pm\frac12}=-\frac{K(h_{j\pm1})+K(h_j)}{2}\times$$
$$\left(\frac{\pm h_{j\pm1}\mp h_j}{\Delta y}-1\right),$$
$$q^y_{i\pm\frac12}=-\frac{K(h_{i\pm1})+K(h_i)}{2}\times$$
$$\left(\frac{h_{i\pm1,j+1}+h_{i,j+1}-h_{i\pm1,j-1}-h_{i,j-1}}{4\Delta y}-1\right),$$
$$q^x_{j\pm\frac12}=-\frac{K(h_{j\pm1})+K(h_i)}{2}\times$$
$$\left(\frac{h_{i+1,j\pm1}+h_{i+1,j}-h_{i-1,j\pm1}-h_{i-1,j}}{4\Delta x}\right),$$
$$D_{1,1,i\pm\frac12}=\left(\alpha_L(q^x_{i\pm\frac12})^2+\alpha_T(q^y_{i\pm\frac12})^2\right)\frac{1}{|\vec{q}_{i\pm\frac12}|}+$$
$$D_o\theta_{i\pm\frac12}$$
$$D_{1,2,i\pm\frac12}=(\alpha_L-\alpha_T)q^x_{i\pm\frac12}q^y_{i\pm\frac12}\frac{1}{|\vec{q}_{i\pm\frac12}|}$$

and analogously

$$D_{2,2,j\pm\frac12}=D_{1,1,i\pm\frac12}\ (i\leftrightarrow j;\alpha_L\leftrightarrow\alpha_T);$$

$$D_{2,1,j\pm\frac12}=D_{1,2,i\pm\frac12}\ (i\leftrightarrow j).$$

4.4 Approximation Scheme for Matrix Temperature

The governing PDE with BC and IC

$$c_m\partial_t T_m-\lambda\Delta T_m=\sigma\theta(T_w-T_m) \qquad (12)$$

$T_m=T_m^k$ is approximated by FVM ((x_i,y_j), $t=t_k$) to

$$c_m\frac{T_m-T_m^{k-1}}{\tau}\Delta x\Delta y$$
$$-\Delta y\lambda\left[\frac{T_{m\ i+1}-T_{m\ i}}{\Delta x}-\frac{T_{m\ i}-T_{m\ i-1}}{\Delta x}\right] \qquad (13)$$
$$-\Delta x\lambda\left[\frac{T_{m\ j+1}-T_{m\ j}}{\Delta y}-\frac{T_{m\ j}-T_{m\ j-1}}{\Delta y}\right]$$
$$=\Delta x\Delta y\sigma\theta^k(T_m-T_w).$$

5 Solution of the Inverse Problem

5.1 Determination of σ and λ

Measuring the temperature of water and matrix in the sample is a difficult task. So we propose the infiltration scenario which enables us to measure σ. There is uniformly distributed small amount of water $h = -100$ in the sample and the initial temperature of water and matrix are the same $T_w = T_m = 20°C$. The vertical boundaries are isolated (zero water and temperature fluxes). The top boundary is free and from the bottom we let water to infiltrate. Water infiltrates by hydraulic pressure from the mantel. The temperature of infiltrating water is $0°C$ We are measuring the water temperature on the top boundary. The model data are the same as data in figure 3. The time evolution of the computed temperature on the top is presented in the figure 4 (blue line).

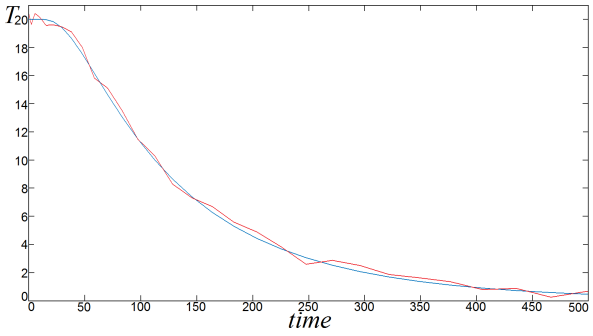

Figure 4: Time evolution of temperature in top of the axis

The computed data have been perturbed by the $0.5°C$ of noise using the random function (green line). These were considered to be measured data. Then, we forgot our transmission coefficient σ $(= 1)$, and matrix heat conduction coefficient λ $(= 0.3)$ and we used an iteration procedure to minimize the discrepancy between the measured data and the computed data.
The optimal point σ_{opt}, λ_{opt} (with respect to the given tolerance) is taken for the required transmission and conduction coefficients. We verify its stability with respect to the choice of starting points in iteration procedure. All measured data correspond to different random noises. During the measured time interval $t \in (0, 500)$ we have used only 31 time moments.

The obtained results with different starting points are collected in Table 1. Used starting points are combinations of $\sigma \in \{0.5, 1.5\}$ and $\lambda \in \{0.1, 0.5\}$. The final value does not depend on the starting point. However, it can be noticed that values of parameters σ, λ slightly mutually interfer. There is always one that is lower than the exact value while the other is changed in a opposite way.

Table 1: Optimal values of λ, σ

start	σ, λ	σ, λ
$[0.5, 0.1]$	$[1.0475, 0.2974]$	$[0.9842, 0.3082]$
$[1.5, 0.1]$	$[0.9547, 0.3277]$	$[1.0212, 0.2945]$
$[0.5, 0.5]$	$[1.0324, 0.2821]$	$[0.9771, 0.3114]$
$[1.5, 0.5]$	$[0.9685, 0.2854]$	$[1.0389, 0.2901]$

5.2 Determination of Dispersion Coefficients

In this case we reduce our system to (3), (4), where we interpret the temperature T_w as the concentration of a tracer. In this case $\sigma = 0$. Our solution domain is cylinder sample (see figure 1) and we consider its vertical cross-section $(0, R) \times (0, Y)$. Here, on the bottom part $r \in (0, R1)$, we consider the outflow

$$QY = K(h(r, 0)), \text{ i.e. } \partial_y h = 0$$

and the rest of the bottom is isolated. The initial saturation of water in the sample corresponds to the $h = -60$ (see (1)) and the concentration is $T_w = 0$. From the cylinder mantle infiltrates water with the constant concentration $T_w = 1$. The rest model data are the same as in previous section. We compute the concentration of the cumulated outflow water and its time evolution is drawn in figure 5. This represents the additional measurement used in the solution of the inverse problem. Determination procedure is the same as before in σ, λ.

The senzitivity of cumulated outflow concentration

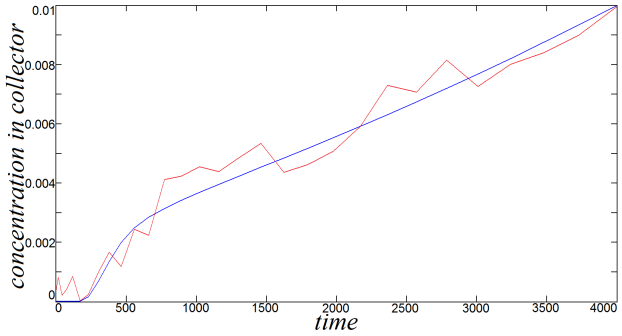

Figure 5: Time evolution of concentration of cumulated outflow water

on dispersion coefficient α_L is drawn in figure 6. The sensitivity of concentration of cumulated outflow water on dispersion coefficient α_T is significantly smaller and its influence on the solution is very small. In our experiment $\alpha_T = \alpha_L/10 = 1/10$. We compute the amount of outflow water using these parameters. Then we perturb it with random noise as can be seen in figure 5 (green line). Then we forget α_L and by means of measurements given by green line we start

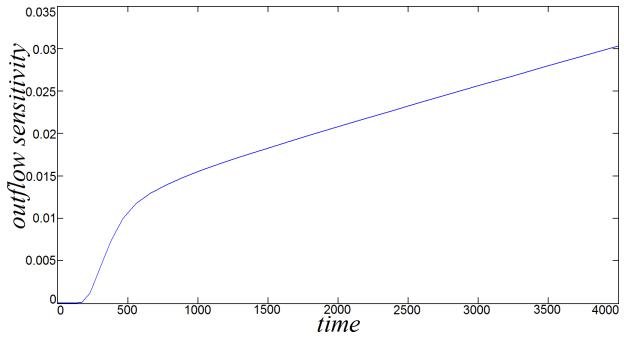

Figure 6: Sensitivity of concentration on dispersion coefficient

the iteration procedure in determination of $\alpha_{L,opt}$. The results are collected in Table 2. At each starting point we consider two different noise perturbations. Each perturbation randomly reaches the value up to one per mile of unite concentration at each time moment of measurements.

Table 2: Optimal values of α_L

start	α_L	α_L
0.5	1.013867	0.997070
1.5	0.993847	1.002343

6 Conclusion

- Numerical modeling of heat exchange arising in water infiltration in unsaturated porous media is discussed.
- Efficient numerical method is developed for heat transport in unsaturated porous media including the heat exchange with the matrix.
- An infiltration scenario is proposed to determine the heat transmission coefficient inside the porous media by solution of inverse problem.
- The developed method is efficient in solving inverse problems in determination of soil parameters, dispersion coefficients and transmission coefficient. Moreover, the suggested experiment scenario could be used also for determination of heat conduction parameter in the matrix.
- General external conditions are prescribed on the boundary.
- The efficiency of the numerical method is demonstrated by numerical experiments.

Acknowledgements: The authors confirm a support by the Slovak Research and Development Agency APVV-15-0681 and VEGA 1/0565/16.

References:

[1] J. Bear, A. H.-D. Cheng "Modeling Groundwater Flow and Contaminant Transport", Springer 2010, V.23 .

[2] D. Constales, J. Kačur: Determination of soil parameters via the solution of inverse problems in infiltration. Computational Geosciences 5 (2004), p. 25-46.

[3] J. Šimunek, M. Šejna, H. Saito, M. Sakai, M. Th. van Genuchten: The Hydrus-1D Software Package for Simulating the Movement of Water, Heat, and Multiple Solutes in Variably Saturated Media. 2013.

[4] J. Šimunek, J. R. Nimo: Estimating soil hydraulic parameters from transient flow experiments in a centrifuge using parameter optimization technique. Water Resour. Res. 41, W04015 (2005).

[5] M. A. Celia, Z. Bouloutas: A general mass-conservative numerical solution for the unsaturated flow equation. Water Resour. Res. 26 (1990), p. 1483-1496.

[6] J. Kačur, P. Mihala, M. Tóth: Determination of soil parameters under gravitation and centrifugal forces in 3D infiltration. Vseas transactions on heat and mass tranfer, Vol. 11, (2016), p. 115-120.

[7] D. Constales, J. Kačur, B. Malengier: A precise numerical scheme for contaminant transport in dual-well flow. Water Resources Research, vol. 39(10), (2003), ..- 1303,

[8] J. Kačur , J. Minár: A benchmark solution for infiltration and adsorption of polluted water into unsaturated-saturated porous media, Transport in porous media, vol. 97, (2013), p. 223-239.

[9] T. L. Bergman, A. S. Lavine, F. P. Incropera, D. P. Dewitt: Fundamentals of heat and mass transfer, John Wiley and Sons, 7th edition, (2011), ISBN 13 978-0470-50197-9.